Ordering and percolation transitions for hard squares: Equilibrium versus nonequilibrium models for adsorbed layers with $c(2\times2)$ superlattice ordering

Da-Jiang Liu
Ames Laboratory, Iowa State University, Ames, Iowa 50011

J. W. Evans
Ames Laboratory and Department of Mathematics, Iowa State University, Ames, Iowa 50011
(Received 18 January 2000; revised manuscript received 7 April 2000)

We study the critical behavior of models for adsorbed layers in which particles reside on a square lattice and have infinite nearest-neighbor repulsions. Such particles are often described as ''hard squares.'' We consider both the equilibrium hard-square model and a nonequilibrium model. The latter involves dimer adsorption onto diagonally adjacent sites, and the desorption and possible hopping of adsorbed monomer particles (where neither adsorption nor hopping can create adjacent pairs of occupied sites). In the limit of high monomer mobility, one recovers the equilibrium model. Both models exhibit a continuous symmetry breaking transition in the Ising universality class, and also a percolation transition for $c(2\times2)$ clusters of particles connected with diagonal bonds. For the equilibrium model, extensive Monte Carlo simulations show that the two transitions coincide, supporting the claim of Hu and Mak. We also determine percolation exponents for $c(2\times2)$ clusters and vacancy clusters, and consider a correlated site-bond percolation problem which elucidates conditions for coincidence of symmetry-breaking and percolation. In contrast, for the nonequilibrium model with immobile adsorbed monomers, there is a gap between the symmetry-breaking and percolation transitions, and the random percolation universality class applies. Finally, we examine the crossover behavior with increasing mobility of adsorbed monomers.

I. INTRODUCTION

A central topic in condensed matter physics is the investigation of phase transitions in lattice models for alloys, spin systems, and commensurate adlayers.[1] In the statistical mechanics literature, a related active area of investigation in recent decades has been the exploration of the relationship between thermodynamic and geometric properties of such *equilibrium* Hamiltonian systems. Motivation for the latter studies comes from the expectation that phase transitions should coincide with the onset of long-range communication, which in turn should coincide with some sort of percolation transition. The challenge is to determine what, if any, definition of ''clusters'' makes the latter coincidence precise. An understanding of these issues can in turn facilitate the design of efficient methods and algorithms to study phase transitions.[2]

Not surprisingly, most work has concentrated on the ferromagnetic Ising model for spin systems. The percolation problem for clusters of sites with the same spin and nearest-neighbor (NN) connectivity (Ising clusters) can be mapped into a dilute q-state Potts model.[3] It has been shown that the percolation transition of such Ising clusters coincides with the Onsager critical point,[4] and that the critical exponents can be extracted from the tricritical $q=1$ Potts model.[5] However, another more complicated definition of clusters (called Ising droplets) is required for percolation and thermodynamic exponents to coincide.[4] There are also some general results for the antiferromagnetic Ising model.[6–8]

Another less traditional area of current interest in statistical physics, which is of relevance here, is the development and analysis of *nonequilibrium* models exhibiting phase transitions. Most previous work focused on models with adsorbing states, together with the analysis of associated ''poisoning'' transitions.[9] However, some recent studies have examined nonequilibrium systems which exhibit Ising-like phase transitions, as well as considering the associated percolation problems.[10,11] Clearly, the same issues arise here as in the analysis of phase transitions in equilibrium systems.

In this study we shall deal exclusively with two-dimensional lattice-gas models that describe commensurately adsorbed layers. Thus, it is appropriate to reformulate the above general comments and issues in the language of these models. Consider first *equilibrium* systems. For a lattice-gas adlayer with NN attractive interactions (the ferromagnetic case), the challenge is to relate phase separation to the percolation of NN clusters of occupied sites. For repulsive interactions (the antiferromagnetic case), one might seek to relate the development of long-range order (i.e., the occurrence of a symmetry-breaking transition) to percolation of checkerboard or $c(2\times2)$ superlattice domains.

Of primary relevance to our work is the limiting case of infinitely strong NN repulsive interactions, where no adjacent pairs of sites can be occupied. This corresponds to the zero-temperature limit of the antiferromagnetic Ising model. For a square lattice of sites, this limit is the equilibrium hard-square (HS) model. The name derives from the feature that allowed configurations correspond to various arrangements of nonoverlapping squares centered on lattice sites and rotated by 45°, with a side length $\sqrt{2}$ times the lattice constant. Although no exact solution to the HS model is available, numerical results (from series expansion, transfer-matrix analyses, etc.) indicate that it belongs to the Ising

universality class.[12–14] There is a symmetry-breaking transition between states with short-range $c(2\times2)$ order at low densities, and long-range $c(2\times2)$ order at high densities. There are also a number of studies relating this transition to the percolation of $c(2\times2)$ domains.[15,8]

The study presented here goes beyond the analysis of the equilibrium HS model to consider a broad class of *nonequilibrium* models that incorporate the former as a limiting case. Thus, our analysis can potentially provide a broader framework within which to elucidate behavior of the equilibrium model. Specifically, we consider an adsorption-desorption model that includes dimer adsorption on diagonal NN sites, and monomer desorption and possible diffusion, subject to infinite NN repulsions. The equilibrium HS model is recovered in the limit of rapid monomer diffusion. Our adsorption-desorption model is motivated by recent treatments of CO oxidation for surfaces characterized by a square lattice of adsorption sites. In these treatments, dissociative adsorption of diatomic oxygen, and diffusion of adsorbed atomic oxygen, are described by the above rules. Desorption of adsorbed oxygen actually occurs only via reaction with highly mobile coadsorbed CO.[16–19]

In Sec. II we present our adsorption-desorption model in more detail, and also discuss some generic properties of systems with $c(2\times2)$ ordering. Then, in Sec. III, we revisit the equilibrium HS model, corresponding to the infinite-mobility limit of our model. We perform extensive Monte Carlo simulations with an efficient cluster algorithm to examine the relationship between the symmetry-breaking and percolation transitions, and calculate the critical exponents for the percolation problem. We also study the percolation of vacancy clusters with NN connectivity (motivated by applications of our model to the study of CO oxidation), and examine a natural site-bond correlated percolation problem. Next, in Sec. IV, we study the zero-mobility limit of our nonequilibrium adsorption-desorption model. We show that the steady state for this model exhibits an ordering transition of the Ising type, similar to the equilibrium HS model. However, its percolation properties are fundamentally different from the HS model. In Sec. V we examine the crossover between the low mobility and high mobility regimes. Finally, in Secs. VI and VII, we provide some general discussion and a summary.

II. DIMER ADSORPTION–MONOMER DESORPTION MODEL WITH $c(2\times2)$ ORDERING

A. Model specification and steady-state behavior

Our adsorption-desorption model involves three processes occurring on a square lattice of adsorption sites: (i) diatomic species (dimers) adsorb dissociatively at each second (or diagonal) NN empty pair of sites at rate $p/2$, provided that the additional six sites adjacent to these are not occupied; this is called the ''eight-site-rule'' since altogether eight empty sites are required for adsorption;[17–19] (ii) adsorbed atoms (monomers) can hop to nearby empty sites, provided that no NN pairs are formed; in general, we can allow NN hops with rate $h_{1NN}/4$, second-NN hops with rate $h_{2NN}/4$, etc. (where these rates refer to each specific final site); (iii) monomers can also desorb at the rate d. Figure 1 illustrates these three types of processes. The above rules ensure that no NN pairs of occupied sites are formed during the process, a feature common in chemisorption systems with very strong NN repulsive interactions between adspecies.

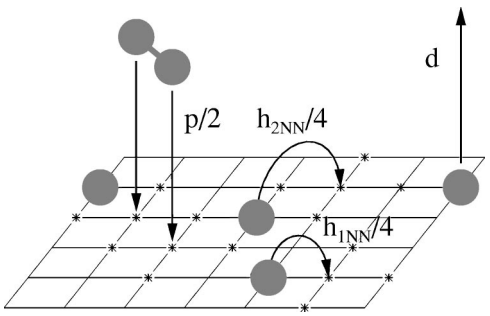

FIG. 1. Schematic of our adsorption-desorption model. For dimer adsorption, the eight sites required to be unpopulated are indicated by *. For two types of monomer hops, sites required to be unpopulated are also indicated by *.

A standard kinetic Monte Carlo algorithm can be used to simulate the general nonequilibrium model. Here, one chooses a site at random and attempts different processes with probabilities determined by their respective rates: $p/(p+d+h_{1NN}+\cdots)$ for dimer deposition, $d/(p+d+h_{1NN}+\cdots)$ for monomer desorption, and $h_{1NN}/(p+d+h_{1NN}+\cdots)$ for monomer hopping to NN sites, etc. An attempt is accepted if it does not violate any constraint. Alternatively, instead of choosing different sites in random, we sometimes use a method that randomly chooses from all possible events.[20] This method has the advantage that it is more efficient when one of the parameter is much larger than the rest, but it involves some ''bookkeeping.'' Note that these two methods are equivalent for infinite systems. We should also mention that more direct and efficient methods are used to simulate the special case of the HS model. Finally, we note that all simulations are performed on $L\times L$ lattices, and employ periodic boundary conditions.

In this study we consider only the steady states of the model. Let θ denote the steady-state coverage, and S_8 denote the ''sticking probability'' that any specific eight-site ensemble required for dimer adsorption is empty. Now, for adsorption to occur at a specific site, the dimer can land in four distinct ways covering that site, each with rate $p/2$, and success probability S_8. Thus, the adsorption rate per site is $2pS_8$. In the steady state, this must match the desorption rate per site of $d\theta$, implying that

$$2pS_8 = d\theta. \tag{1}$$

In this relation, both S_8 and θ depend on p and d, as well as on the monomer hopping rates, h_{iNN}.

In the limit of high monomer hopping rates, $h_{iNN}\to\infty$, rapid diffusion of adsorbed particles (on the time scale of adsorption and desorption processes) ensures that the adlayer is equilibrated. This claim relies on the fact that our hop rates satisfy detailed balance for infinite NN repulsions, and the feature that our general hopping dynamics allows all configurations to be sampled. This equilibrium state corresponds to the HS model, with the coverage θ being determined by the ratio p/d. Note that if monomer diffusion were to occur only through NN hopping, then it would be highly restricted at high coverages.[21] In this situation, it is possible that a

''blocking transition'' could occur at high coverages preventing the system from becoming equilibrated. See below and Appendix A.

For a given choice of monomer mobility h_{iNN} and desorption rate d, it is clear that the steady-state coverage θ in our model increases monotonically from 0 as p increases from 0 to ∞. For convenience, we define a reduced dimer deposition rate $u=p/(p+d)$. Then, θ increases monotonically as u increases from 0 to 1. For the HS model ($h_{\mathrm{iNN}}\to\infty$), one has $\theta(u\to 1)=1/2$. For immobile monomers ($h_{\mathrm{iNN}}=0$), one has $\theta(u\to 1)\approx 0.425\,34$. This nontrivial behavior, which persists for finite $h_{\mathrm{iNN}}\neq 0$, is discussed in Appendix A. Behavior of θ near the ordering transition (defined in the following sections) is examined in Appendix B. Finally, we note that for lower θ, a moderate amount of NN hopping of monomers suffices to effectively equilibrate the adlayer. However, for high θ, such diffusional dynamics is highly constrained, and equilibration is limited. See Fig. 2 of Ref. 19.

As indicated in the Introduction, our adsorption-desorption model is actually motivated by recent lattice-gas modeling of the catalytic CO oxidation on surfaces. The Langmuir-Hinshelwood mechanism for this reaction involves adsorption of CO onto single empty sites; adsorption of oxygen (O_2) onto suitable empty pairs of sites; and the reaction of adjacent adsorbed CO and oxygen. In the modeling, adsorption sites were assumed to form a square lattice, and dissociative adsorption of diatomic oxygen was according to the ''eight-site-rule.'' Possible subsequent diffusion of adsorbed oxygen was sometimes included with the constraint that no adjacent pairs of this species could be created. (Both the adsorption and diffusion rules reflect the presence of very strong NN repulsions between adsorbed oxygen.) In the modeling adsorbed CO was assumed highly mobile, and CO-CO and CO-oxygen interactions were ignored, implying that CO is randomly distributed on sites not occupied by adsorbed oxygen.[16–19] Consequently, if one focuses on the dynamics of the oxygen adlayer, it is described by our adsorption-desorption model, with the CO coverage acting as a mean-field parameter controlling the desorption rate. This connection is important in motivating some aspects of the following study.

B. General characterization of $c(2\times 2)$ ordering

In the presence of infinite NN repulsions, adsorbed particles tend to form checkerboard or $c(2\times 2)$ domains. See Fig. 2. The particles in a single such domain are connected by diagonal bonds, and occupy one of the two $(\sqrt{2}\times\sqrt{2})R45°$ sublattices composing the full square lattice. These sublattices are labeled below by $+$ and $-$, and domains on different sublattices are usually described as having different phases. In general, particles can reside on both sublattices (these are distinguished by filled and empty circles in Fig. 2). Thus, one has $\theta=\theta_+ + \theta_-$, where $\theta_\pm$ are the fractional coverages on the two sublattices. At low coverages when the system is disordered, one has $\theta_+=\theta_-$ for an infinite lattice. However, at higher coverages, one expects a spontaneous symmetry breaking with $\theta_+\neq\theta_-$. Indeed, at the maximum coverage of $\theta=1/2$, one sublattice must be completely occupied, and the other must be empty. The transition also corresponds to the establishment of long-range $c(2\times 2)$ order, and is also referred to as an order-disorder transition.

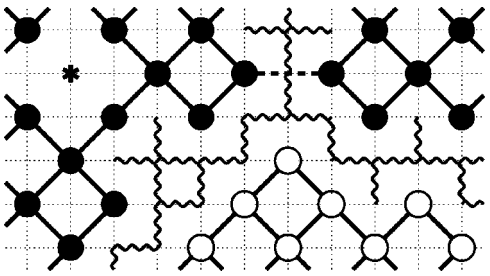

FIG. 2. $c(2\times 2)$ domain structure. Solid bonds denote 2nd NN domains. The two 2nd NN domains at the top, joined by a dashed bond, form a single 3rd NN domain. Empty and filled circles denote particles on different $c(2\times 2)$ sublattices. A NN vacancy domain dual to the 2nd NN $c(2\times 2)$ domains, which also corresponds to a domain boundary, is shown by the wiggly bonds. * denotes an ''isolated defect.''

In our analysis of steady-state behavior, we define an order parameter $m=\theta_+-\theta_-$, and then expect that $\langle|m|\rangle \sim(\theta-\theta_c)^\beta$, for $\theta\to\theta_c^+$, if the system exhibits a second-order phase transition at θ_c. Here, $\langle\cdots\rangle$ denotes the ensemble average. Other physical quantities which should exhibit singular behavior include fluctuations of the order parameter $\langle m^2\rangle\sim(\theta-\theta_c)^{-\gamma}$, and the spatial correlation length $\xi\sim(\theta-\theta_c)^{-\nu}$. The three exponents satisfy a generic scaling relation $\mathrm{d}\nu=2\beta+\gamma$, where $\mathrm{d}=2$ is the lattice dimension.

Next, we discuss in more detail issues of domain structure and percolation. One can precisely define $c(2\times 2)$ domains as clusters of particles with specific connectivity rules. There are two natural choices. The first is second-NN connectivity, where two particles that are second nearest neighbor (2nd NN) to each other are in the same cluster. The second choice is second NN + third NN (or just 3rd NN, for short) connectivity, where particles forming either 2nd NN or 3rd NN pairs are in the same cluster. We shall also consider clusters of unoccupied sites with NN connectivity (NN vacancy clusters). See Fig. 2 for examples. Note that NN vacancy clusters are ''dual'' to 2nd NN particle clusters, in the sense that either one or the other (but not both) percolate (for an infinite lattice). This type of duality can be formulated more precisely in terms of ''matching lattices'' from graph theory.[22] We emphasize that there is no such relationship between NN vacancy clusters and 3rd NN particle clusters.

As far as we are aware, there are no previous detailed studies of the properties of NN vacancy clusters in models with $c(2\times 2)$ ordering. Our motivation for such studies is twofold. The first is purely geometrical, noting that at higher coverages, the NN vacancy clusters reflect the structure of antiphase or domain boundaries [which separates $c(2\times 2)$ domains of different phases]. The second motivation comes from the consideration of models for CO oxidation described at the end of Sec. II A, where adsorbed oxygen forms $c(2\times 2)$ domains. Suppose the dominant diffusion process for coadsorbed CO is hopping to adjacent empty sites. Then, CO diffusion is effectively restricted to (and relies on the percolation of) NN vacancy clusters.[19]

For a continuous percolation transition, the probability P_∞ that a particle belongs to the infinite cluster is expected to

behave like $P_\infty \sim (\theta - \theta_p)^{\beta_p}$ as $\theta \to \theta_p$, where θ_p is the percolation threshold. Other singular quantities include the average cluster size, defined as $s_{\rm av} = \Sigma_s s^2 n_s / \Sigma_s s n_s$, where n_s is the density of clusters with exactly s particles, and the connectivity length ξ_p defined as the average separation between particles in one cluster. We denote the critical exponents for $s_{\rm av}$ and ξ_p by γ_p and ν_p, respectively. Analogous to symmetry breaking, one has the scaling relation $d\nu_p = 2\beta_p + \gamma_p$, with $d=2$. Exactly at the percolation point, the infinite cluster has fractal dimension $d_f = d - \beta_p/\nu_p$, where $d=2$ is again the lattice dimension.

There is a direct connection between symmetry breaking and the percolation of a $c(2\times 2)$ domain: from simple topological arguments, one can deduce that percolation cannot occur without symmetry breaking. Suppose that domains on the + sublattice percolate (for either of the above choices of connectivity) while there is no symmetry breaking. This would block percolation of domains on the − sublattice (cf. Fig. 2), violating the presumed lack of symmetry breaking. Thus, the critical coverage for the symmetry-breaking transition cannot exceed the percolation coverage.[23] Thus, we have two scenarios for a system of particles with infinite NN repulsions that exhibits continuous symmetry-breaking and percolation transitions: $\theta_p > \theta_c$ (A), or $\theta_p = \theta_c$ (B). For scenario A, one expects that the percolation transition belongs to the random percolation universality class. For scenario B, due to the divergent correlation length, the percolation transition can belong to a new universality class.

III. THE EQUILIBRIUM HARD-SQUARE MODEL (INFINITE SURFACE MOBILITY)

In the following, rather than using the reduced dimer deposition rate u, defined in Sec. II A, we more conventionally analyze hard-square (HS) model properties in terms of an activity z, associated with the grand canonical ensemble, i.e., each configuration with n particles has a weight z^n. [If one generates HS model configurations as steady states of a model with both monomer adsorption (subject to NN exclusion) and desorption, then z also corresponds to the ratio of rates for these processes.] Since larger z puts more weight on configurations with a larger number of particles, it thus corresponds to higher coverage, and higher u. The relation between z and u is nontrivial, but can be obtained by substituting the form of $\theta = \theta(z)$, and $S_8 = S_8(z)$, into Eq. (1). We expect that the relation between θ and z (or u) has at most a logarithmic singularity at the ordering transition. See Appendix B. Thus the critical exponents describing the divergence of various quantities are independent of whether the quantity is regarded as a function of θ or z.

Despite its simplicity, the equilibrium hard-square (HS) model for particles with infinite NN repulsions on a square lattice has not yet been solved exactly. The ordering transition for this model has been studied using several numerical techniques, e.g., series expansion,[24] Monte Carlo simulations,[25] corner transfer matrix,[26] and transfer-matrix finite-size scaling (TMFSS).[27,12] The numerical values for the critical point and exponents can be obtained most accurately using the TMFSS method: the best estimates are $z_c = 3.796\,255\,174(3)$ for the critical activity,[28,29] and $\theta_c = 0.367\,743\,000(5)$ for the critical coverage.[28,14] The critical exponents are consistent with Ising values (to high precision).

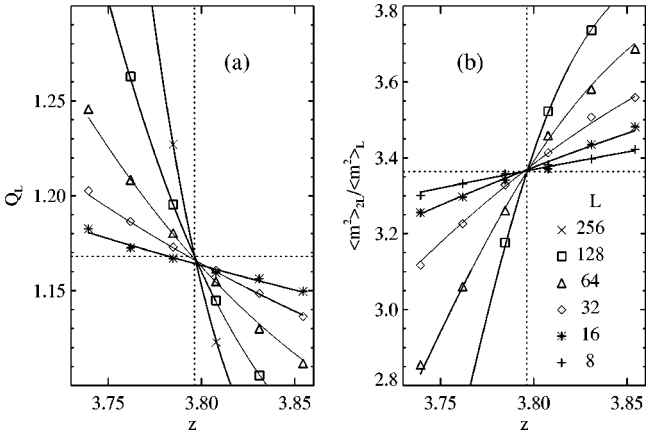

FIG. 3. Q_L (a) and $\langle m^2\rangle_{2L}/\langle m^2\rangle_L$ (b) versus activity z for the hard-square model. The vertical dotted line indicates $z_c = 3.796\,26$ and the horizontal dotted line indicates $Q_c = 1.1679$ (a) and $2^{7/4}$ (b), respectively. System size for each curve is indicated on the right panel.

Based on Monte Carlo simulation data, Hu and Mak[15] argued that there is a coincidence between the ordering and percolation transitions in the hard-square model, for both 2nd NN and the 3rd NN connectivity (cf. Fig. 2). This supported an earlier claim by Binder and Landau.[25] Their observation of a coincidence extended to a variety of other systems with hard-core interactions.[15] The coincidence for the hard-square model for 3rd NN connectivity has in fact been established rigorously,[7,8] but the same is not true for 2nd NN connectivity (which is more relevant for our applications).

In this section we report Monte Carlo simulation data from our finite-size scaling study. A significant difference from previous work is our employment of a cluster algorithm for the hard-square model which greatly improves the efficiency near the critical point. The algorithm is motivated by the work of Dress and Krauth[30] for hard-core gas in continuous space, and is described in Appendix C. We also report a variety of results regarding percolation properties.

A. Ordering transition

Here we report results for the ordering transition in the hard-square model. They mainly serve two purposes. One is to test the efficiency of our cluster algorithm in generating equilibrium configurations, particularly near the transition. The other is to gauge corrections to finite-size scaling at the ordering transition, for comparison with analyses of the nonequilibrium model (for which we will apply identical procedures).

One of the most accurate ways to determine critical points for phase transitions is via analysis of the fourth-order cumulant of the order parameter.[31] This quantity for an $L\times L$ lattice is sometimes defined as

$$Q_L = \langle m^4\rangle / \langle m^2\rangle^2, \tag{2}$$

with $m = \theta_+ - \theta_-$ as above. Figure 3(a) shows Q_L versus z for $L = 16$, 32, 64, 128, and 256. Symbols indicate the results of simulations performed for a specific z value and system

size L. For each system size, a multiple histogram method[32] is used to draw continuous lines for varying z. Finite-size scaling theory predicts that as $L\to\infty$, various curves should cross at the same point (z_c,Q_c). The vertical dotted line indicates the critical activity z_c, and the horizontal dotted line indicates Q_c (which adopts a universal value for a specific boundary condition), both obtained using the TMFSS method.[29,33] As can be seen from the figure, the agreement is quite good, and corrections to finite-size scaling are relatively small. As an independent test of the universality class (and our algorithm), we estimate the critical point using a cell-to-cell renormalization, requiring $Q_L(z^*)=Q_{2L}(z^*)$. From data for $L=64$ and 128, we obtain $z^*=3.7965(4)$ and $Q_c=1.1667(5)$.

We can use other quantities to locate the critical point by assuming a finite-size scaling ansatz. Suppose some physical quantity P scales as $(z-z_c)^{-\rho}$ in an infinite system near the critical point z_c. Then, the finite-size scaling theory predicts that it has the following scaling form for a system of size $L\times L$

$$P_L\sim L^{\rho/\nu}F((z-z_c)L^{1/\nu}), \tag{3}$$

where ν is the critical exponent for the characteristic length, and $F(x)\sim x^{-\rho}$, as $x\to\infty$. There are several ways of using the above equation to extract critical properties. If z_c is known, one can estimate ρ/ν using data for P_L at z_c for different system sizes. If ρ/ν is known, then one can plot $L^{-\rho/\nu}P_L$ versus z, and determine z_c in the same way as using the cumulant. If neither z_c nor ρ/ν is known, one can use three different system sizes to determine z_c and ρ/ν simultaneously. One way to do this is by plotting $P_{bL}(z)/P_L(z)$ versus z for different L. From Eq. (3) these curves should cross at $(z_c,b^{\rho/\nu})$. Figure 3(b) is such a plot for $P=\langle m^2\rangle$, where $\rho=\gamma$, and the susceptibility exponent γ equals to 7/4 for the Ising universality in 2D. Again the finite-size scaling ansatz is satisfied with relatively small corrections. Using systems of size $L=64$, 128, and 256, we estimate $z_c=3.7962(9)$ and $\gamma/\nu=1.749(3)$. A similar plot (figure not shown) has been made for $P=\langle|m|\rangle$ which give $z_c=3.7964(3)$ and $\beta=0.1252(6)$. The exact value for β for the 2D Ising model is 1/8.

B. Percolation of $c(2\times2)$ domains

Above, we noted that previous simulations suggest a coincidence of the percolation and ordering transitions for the hard-square model,[15] but this has only been shown rigorously for 3rd NN connectivity. Here we report a more extensive Monte Carlo study of this issue, and determine the percolation exponents. Our results support the claim of coincidence of the ordering transition and the percolation transition for both 2nd and 3rd NN connectivity.

To determine the percolation point, we calculate the probability R that there exists a cluster spanning from one side of the lattice to the other along a major axis. We use free boundary conditions in the definition of clusters (but periodic boundary conditions in the HS model simulations). R is expected to exhibit a similar property as the cumulant Q for the ordering transition: R_L versus z curves, for lattices of different linear sizes L, should approach a step function, as $L\to\infty$. For the random percolation universality class, it has been shown that the R value of the crossing point of these curves approaches $R_c=1/2$, as $L\to\infty$.[34] Figure 4 shows the $R_L(z)$ curves for the hard-square model with 2nd NN connectivity. The correction to finite-size scaling is quite large compared to the ordering transition and the random percolation problem. The crossing point between different R_L curves shifts to a value very close to 1, as L increases, in sharp contrast to random percolation.

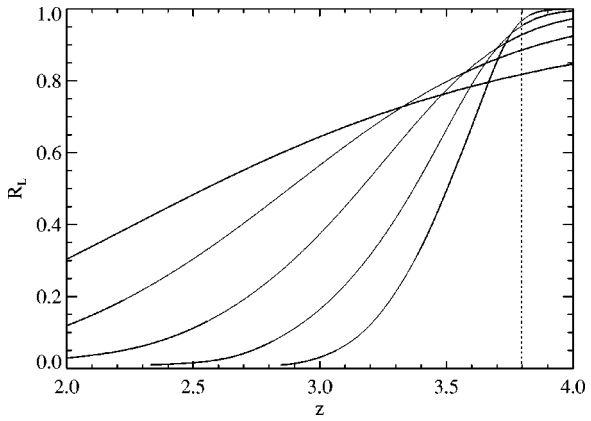

FIG. 4. R_L versus z with the lines are drawn using the histogram method. Curves with increasing steepness correspond to $L=8$, 16, 32, 64, and 128. Results for z_L^* are obtained from the crossing points. The vertical dotted line indicates the critical activity z_c for the ordering transition.

We obtain a finite-size estimate z_L of the percolation point using the ''cell-to-cell'' renormalization-group method by requiring that $R_L(z_L^*)=R_{bL}(z_L^*)$. Results are shown in Fig. 5. To extrapolate to the $L\to\infty$ limit, we assume the following form for finite-size corrections:

$$R_L(z)=R_c+b_0(\log L)/L+b_1/L+(z-z_p)\times(a_0L^{1/\nu_p}+a_1\log L)+\cdots, \tag{4}$$

where $1/\nu_p$ is the exponent for the connectivity length for the percolation problem. Note that, in general, ν_p can be different from the correlation length exponent $\nu=1$ for the ordering transition. From Eq. (4) one can see that z_L^* should have the following finite-size correction form:

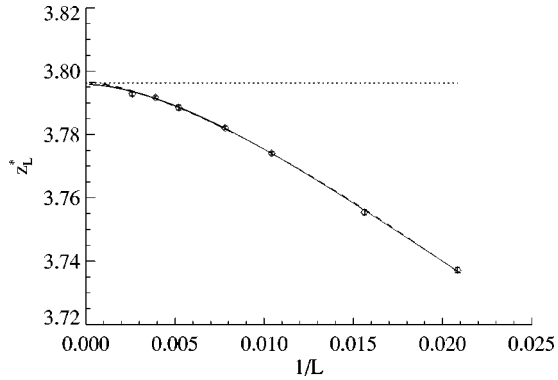

FIG. 5. z_L^* versus $1/L$ obtained through cell-to-cell renormalization using the spanning probability for the 2nd NN clusters. The solid line is a fit using $\nu_p=1$, and the dashed line is a fit using $\nu_p=4/3$. The horizontal dotted line indicates the critical activity z_c for the ordering transition.

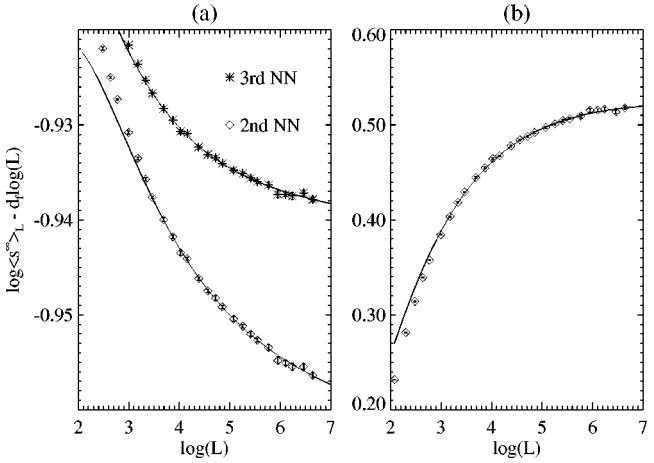

FIG. 6. (a) Log$\langle s^{\infty}\rangle$ versus log L (subtracting the Ising behavior $d_f^{\mathrm{Ising}}\log L$), for 2nd NN and 3rd NN connectivity. Solid lines are fit to Eq. (6) with logarithmic corrections. (b) Similar plot for the NN vacancy cluster, with $d_f=1.39$.

$$z_L^*=z_p+c_0(\log L)/L^{1+1/\nu_p}+c_1/L^{1+1/\nu_p}. \tag{5}$$

Using $\nu_p=1$ and results in Fig. 5, through least-square fitting, we obtained $z_p=3.7959(5)$, which coincides to high precision with $z_c=3.796\,25$.[29] If $z_p\neq z_c$, ν_p is likely to be 4/3, the random percolation value. In order not to bias against this possibility, we also fit the data with $\nu_p=4/3$, and obtained $z_p=3.7966(6)$. See Fig. 5. Note that different assumptions for corrections to finite-size scaling should yield the same z_p in the limit that $L\to\infty$.

Our numerical study of spanning probability behavior (which is much more extensive than previous work) strongly suggests that the percolation transition for 2nd NN connectivity coincides with the ordering phase transition for the HS model. This supports the claim of Hu and Mak.[15] The analysis below on the critical exponents suggests that they deviate significantly from random percolation values, consistent with such a coincidence. However, based on these studies, one cannot exclude the possibility that there is a very small gap between z_p and z_c. With this in mind, we refer the reader to the study in Sec. III D, which perhaps provides the most compelling evidence for coincidence.

Hu and Mak[15] also suggested that scaling behavior for percolation in the HS model should reflect the Ising universality class. Indeed, it is almost certain that $\nu_p=\nu=1$ (if percolation indeed coincides with the ordering transition). Using a formal argument, Stella and Vanderzande[5] show that the exponents for Ising clusters (i.e., clusters of up spins with NN connectivity in the standard Ising model) are those of the tricritical $q=1$ Potts model, which imply a fractal dimension of $d_f=\frac{187}{96}$, and an exponent for the average cluster size of $\gamma_p=\frac{91}{48}$. To analyze percolation exponents in the HS model, we measure the number of sites belonging to each cluster, for both 2nd NN and 3rd NN connectivity at $z=z_c$. Figure 6(a) is a log-log plot of data for the largest cluster size $\langle s^{\infty}\rangle$ versus L. To highlight the finite-size correction to the power-law behavior, we subtract from $\log\langle s^{\infty}\rangle$ the scaling behavior, $\frac{187}{96}\log(L)$, the predicted scaling form of this quantity for Ising clusters.

To more precisely analyze the data, we assume a similar form for the finite-size correction as in Eq. (4). Thus, when $z=z_c=z_p$, we write

$$\langle s^{\infty}\rangle\approx L^{d_f}[a_0+a_1(\log L)/L+a_2/L]. \tag{6}$$

Fitting data from $L=48$ to 768 based on this form, we obtain $d_f(2\mathrm{NN})=1.946\pm0.001$ for the 2nd NN connectivity, and $d_f(3\mathrm{NN})=1.947\pm0.001$ for the 3rd NN connectivity. These results may suggest slightly different values for $d_f(2\mathrm{NN})$, $d_f(3\mathrm{NN})$, and the value of $d_f=\frac{187}{96}\approx1.9479$ for Ising clusters. However, it is quite possible that all three are identical, considering the uncertainty in the form of finite-size corrections and the subjective choice of the range of fitting.

In a similar analysis, we measured the exponent γ_p for the average cluster size (normalized by ν_p). Figures are not included. We obtained $\tilde{\gamma}_p=\gamma_p/\nu_p=1.893(2)$ for 2nd NN connectivity, and 1.895(2) for 3rd NN connectivity. In comparison the value for Ising cluster is $\tilde{\gamma}_p=91/48\approx1.8958$. Our results for percolation exponents are also consistent (to high precision) with the scaling relation $\tilde{\gamma}_p=2d_f-\mathrm{d}$ (with $\mathrm{d}=2$), obtained from the relations listed in Sec. II B.

C. Percolation of NN vacancy clusters

Next, we consider the percolation properties of vacancy clusters with NN connectivity. As noted in Sec. II B, these are ''dual'' to $c(2\times2)$ domains with 2nd NN connectivity, so their percolation transitions coincide. Exploiting the analogous duality property, recently Bastiaansen and Knops[35] argued that the fractal dimension for clusters with 2nd NN connectivity in the ferromagnetic Ising model adopts the same Ising value as for clusters with NN connectivity. However, unlike the ferromagnetic Ising model, there is no particle-vacancy symmetry for the HS model at the critical point. Indeed, we find that the fractal dimension for NN vacancy clusters in the HS model is much smaller than both that for 2nd NN $c(2\times2)$ particle domains (which is close or equal to the Ising value), or the random percolation value. Figure 6(b) shows the size dependence for the largest cluster size versus system size. Using data from $L=48$ to 768, and the logarithmic correction term in Eq. (6), we obtain $d_f=1.388(6)$. The finite-size correction is much larger for the NN vacancy clusters than for the particle clusters. [Note the range of the y axis in Fig. 6(b).] Similarly, we estimate that $\tilde{\gamma}_p=0.792(7)$ for the NN vacancy clusters, again consistent with the scaling relation $\tilde{\gamma}_p=2d_f-\mathrm{d}$ (with $\mathrm{d}=2$).

To obtain an intuitive understanding of our results, we show in Fig. 7 a ''typical'' real-space configuration of 2nd NN particle clusters, and NN vacancy clusters, near the ordering transition in the HS model. The vacancy cluster appears much more one-dimensional than the particle clusters. A cursory look at the picture suggests that the vacancy cluster constitutes the exterior perimeter (i.e., the ''hull'') of the particle cluster. Vanderzande and Stella[36] showed that the hull fractal dimension for the 2D ferromagnetic Ising clusters is 11/8=1.375. This value is in close agreement with, but smaller than, our best estimate of the fractal dimension for NN vacancy clusters. Indeed, as can be seen from closer examination of Fig. 7, the largest vacancy cluster does not

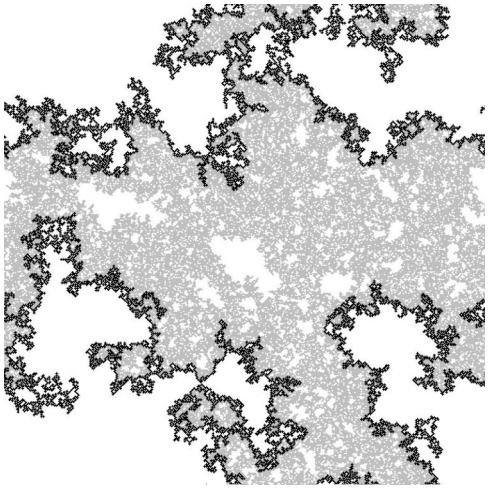

FIG. 7. A snapshot of the largest 2nd NN particle cluster (gray), and NN vacancy cluster for vacancies (black), for the HS model at the critical point. The system size is 512×512 and we use the periodic boundary condition in both directions.

exactly follow the exterior perimeter of the largest particle cluster. There are occasional excursions away from the perimeter into regions which are in fact populated by different particle clusters (not shown in this picture). If these excursions occur with all sizes, then the fractal dimension of vacancy clusters can be different from the hull fractal dimension of the particle clusters. However, due to the uncertainty in the form of finite-size corrections and the limited range of L, we cannot exclude the possibility that d_f may indeed be 11/8.

D. Site-bond correlated percolation

It is natural to examine whether the coincidence of ordering and percolation transitions of $c(2\times2)$ domains in the HS model persists not just for 3rd NN and 2nd NN connectivity, but also for shorter range choices of connectivity. In fact, one can reduce the range of connectivity continuously from the 2nd NN case by introducing an activation probability, $p\leqslant1$, for diagonal bonds (i.e., we connect two occupied 2nd NN sites with probability p). Of course, $p=1$ recovers the standard choice of 2nd NN connectivity.

In our analysis we fix the activity for the HS model at the known critical value, and then adjust p to find the critical value for this parameter, i.e., the value where percolation first occurs at this activity. Figure 8 shows the spanning probability R versus p for the HS model at z_c. From the crossing point, we estimate that $p_c\approx0.70$. The FSS of $\langle s^{\infty}\rangle$ and $\langle s_{\mathrm{av}}\rangle$ show percolation exponents close to the Ising critical exponent $\beta=1/8$ and $\gamma=7/4$. In other words, these site-bond correlated clusters with $p=p_c$ constitute ''Ising droplets'' for the HS model. The fact that $p_c<1$ means that percolation occurs at the ordering transition for a range of $p_c\leqslant p\leqslant1$. We take this as compelling evidence that there is no gap between the ordering and percolation transitions for 2nd NN connectivity ($p=1$), an issue to which we return in Sec. VI.

IV. THE NONEQUILIBRIUM ADSORPTION-DESORPTION MODEL WITH ZERO SURFACE MOBILITY

In this section we consider both the ordering and percolation properties of the zero-mobility limit of the nonequilibrium model. The techniques of analysis are the same as those applied for the HS model, facilitating a direct comparison of behavior of these models. Below, it is convenient to consider quantities as functions of u rather than of coverage. The relationship between u and coverage is assumed to have at most logarithmic singularities at the ordering transition. See Appendix B. Consequently, the critical exponents are independent of whether the quantity is regarded as a function of coverage, or of u.

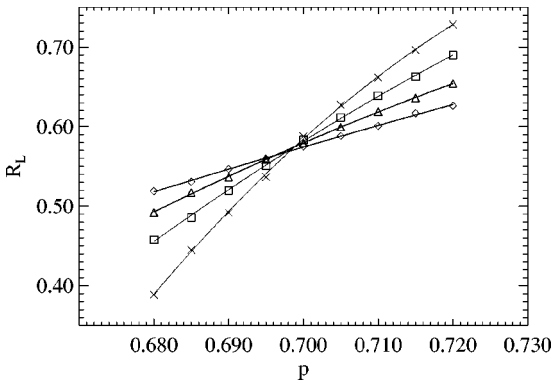

FIG. 8. Spanning probability in the site-bond correlated percolation problem for the HS model at z_c. Curves with increasing steepness corresponds to $L=32$, 64, 128, and 256.

A. Ordering transition

To study the ordering behavior of the nonequilibrium model, we use the same finite-size scaling technique as described in Sec. III A. We perform Monte Carlo simulations on systems of size $L=8$, 16, 32, and 64. Simulations were typically over 5×10^6 Monte Carlo sweeps (MCS). A site is visited once on average for each MCS which corresponds to $(p+d)^{-1}$ in physical time. The first 10^6 MCS of data were discarded to allow ample time for the system to reach steady state.

We first use the fourth-order cumulant Q_L [Eq. (2)] of the order parameter to locate the critical point of the order-disorder phase transition. As in equilibrium models undergoing continuous phase transitions, Q_L for different L tend to cross at the same point as L approaches infinity. Using $L=32$ and 64, we obtain $u_c\approx0.7139(4)$. The corresponding Q value is 1.165(3), consistent with the value for the Ising universality class.[33] The corresponding value obtained for the critical coverage is $\theta_c=0.296(1)$, well below the value for the HS model. See Fig. 3(a) in Ref. 19.

Critical exponents for the ordering transition can be obtained using the finite-size scaling procedures described in Sec. III A [i.e., using Eq. (3) replacing the variable z by u]. We show the simulation results for $P=\langle|m|\rangle$ versus u in Fig. 9. Using results for $L=16$, 32, and 64, we estimate that $u_c=0.7138(7)$ (Fig. 9), in good agreement with the result obtained using the cumulant. From the ordinates of the crossing point we estimate the critical $\beta/\nu=0.123(5)$ (Fig. 9). A similar analysis using $P=\langle m^2\rangle$ yields $u_c=0.7138(6)$ and $\gamma/\nu=1.753(8)$ [cf. Fig. 3(b) of Ref. 19].

Equation (3) (with z replaced by u) also implies that

$$C_L(u_c)=\frac{\partial}{\partial u}\ln P_L(u_c)\sim L^{1/\nu}. \tag{7}$$

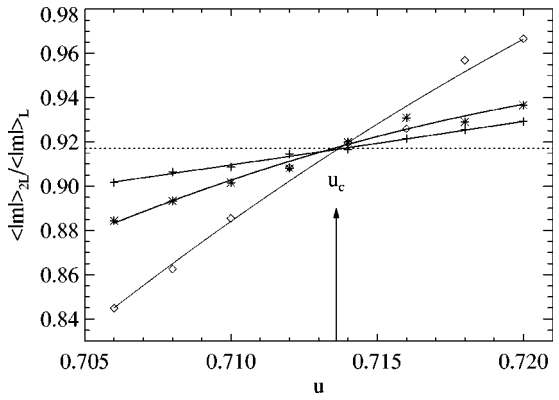

FIG. 9. $\langle|m|\rangle_{2L}/\langle|m|\rangle_L$ versus u for $L=8$, 16, and 32 for the nonequilibrium model with $h_{\mathrm{iNN}}=0$. The dotted horizontal line indicates the value $2^{-1/8}$.

Using this approach, we estimate $\nu=0.98(2)$ for $L=8$ to 64. All these exponents agree very well with the 2D Ising critical exponents ($\beta=1/8$, $\gamma=7/4$, and $\nu=1$) and suggest that the ordering phase transition of the adsorption-desorption model with $h_{\mathrm{iNN}}=0$ belongs to the Ising universality class.

B. Percolation transitions

Figure 10 shows simulation results for the size of the largest cluster s^{∞} versus u, for $c(2\times2)$ particle domains with 2nd NN connectivity in the adsorption-desorption model with $h_{\mathrm{iNN}}=0$. Using the same cell-to-cell renormalization-group method as described in Sec. III B, we estimate that $u_p^{2\mathrm{NN}}=0.727(1)$. We did not try to account for any corrections to finite-size scaling, but we believe these should be smaller than the statistical error. In Ref. 19 we use spanning probability R_L and obtain the same percolation transition point. By plotting R_L versus the steady-state coverage θ, we estimate the percolation coverage $\theta_p^{2\mathrm{NN}}$ to be 0.305(1).

Thus, by comparison with our results on ordering from Sec. IV A, we conclude that there is a gap between the ordering transition and the percolation transition for $c(2\times2)$ particle domains with 2nd NN connectivity in this nonequilibrium model. This is in contrast to the situation for the hard-square model. While the gap is small (about 1% in coverage), it is clearly resolved given the statistical precision of our study. In Fig. 10 we indicate our estimate of the two

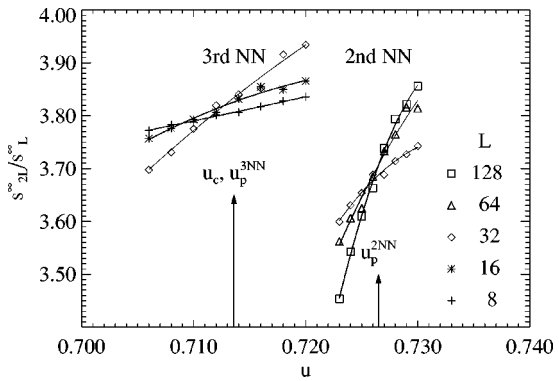

FIG. 10. FSS for the size of the largest $c(2\times2)$ cluster with the 3rd NN connectivity for the nonequilibrium model with $h_{\mathrm{iNN}}=0$.

TABLE I. Finite-size scaling estimates of percolation exponents for $c(2\times2)$ domains with 2nd NN connectivity in the adsorption-desorption model with $h_{\mathrm{iNN}}=0$. The ''exact'' results for random percolation are $\tilde{\beta}_p=\beta_p/\nu_p=5/48\approx0.1042$, and $\tilde{\gamma}_p=\gamma_p/\nu_p=43/24\approx1.792$. Reported estimates correspond to the crossing point of curves for P_{2L}/P_L versus u, and $P_L/P_{L/2}$ versus u. We choose P as the probability of being in the spanning cluster (the average cluster size) for estimates of $\tilde{\beta}_p$ ($\tilde{\gamma}_p$).

L	u_p	$\tilde{\beta}_p$	u_p	$\tilde{\gamma}_p$
16	0.7250(5)	0.140(1)	0.730(1)	1.791(3)
32	0.721(1)	0.161(2)	0.725(2)	1.747(6)
64	0.7254(5)	0.128(4)	0.726(1)	1.76(1)
128	0.7265(10)	0.109(6)	0.7269(13)	1.786(15)

transitions by arrows, and they are clearly separated beyond statistical uncertainties. One consequence of this gap is that the percolation transition $c(2\times2)$ domains with 2nd NN connectivity in the nonequilibrium model with $h_{\mathrm{iNN}}=0$ belongs to the random percolation universality class.

Table I lists our results for various percolation exponents for $c(2\times2)$ domains with 2nd NN connectivity, which were extracted using the finite-size scaling method. Note the large and irregular finite-size corrections. We attribute this effect to the presence of an ordering transition in close proximity to the percolation transition. However, our results are consistent with random percolation values.

For the nonequilibrium model with $h_{\mathrm{iNN}}=0$, is there also a gap between the ordering transition and the percolation transition for $c(2\times2)$ domains with 3rd NN connectivity? To address this issue, in Fig. 10 we also show results for the 3rd NN connectivity. As can be seen from the figure, the crossing points lie very close the ordering phase transition point. Moreover, the y-axis crossing value, which is related the percolation exponent, is very different from the prediction from the random percolation universality class. This suggests that the percolation transition with 3rd NN connectivity is shifted to a different universality class by virtue of coincidence with the ordering transition.

From duality, the percolation transition for NN vacancy clusters should occur at $u=u_p^{2\mathrm{NN}}$. Thus, it is distinct from the ordering transition at $u=u_c$ for the nonequilibrium model with $h_{\mathrm{iNN}}=0$, and should belong to the random percolation universality class. Estimation of critical exponents for NN vacancy clusters (not shown) supports this claim. For comparison with the hard-square model, we show in Fig. 11 a ''typical'' real-space configuration of 2nd NN particle clusters, and NN vacancy clusters, near the ordering transition of the nonequilibrium model with $h_{\mathrm{iNN}}=0$ at $u=0.727$. Since for this nonequilibrium model, the ordering transition happens at a much lower coverage than in the HS model, there are numerous ''holes'' in typical $c(2\times2)$ domains. Consequently, the vacancy clusters exhibit very large excursions from the perimeter of the $c(2\times2)$ domains (in comparison with the HS model, where the vacancy clusters exhibit a substantially smaller fractal dimension).

V. TRANSITION OUT OF THE ZERO-MOBILITY LIMIT

A basic question is how does ordering and percolation behavior change from that described in Sec. IV as one intro-

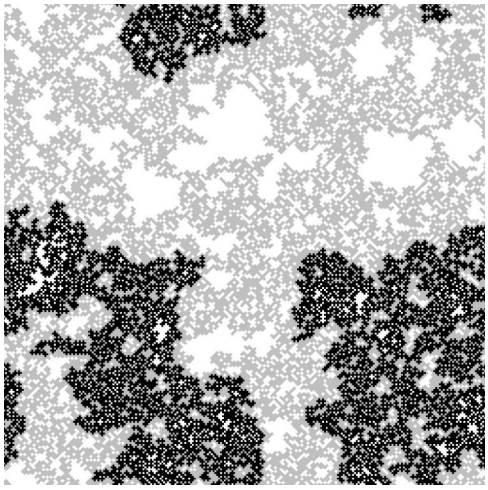

FIG. 11. A snapshot of the largest 2nd NN particle cluster (gray) and NN vacancy cluster for vacancies (black) for the nonequilibrium model with $h_{\mathrm{iNN}}=0$ at the critical point $u=0.727$. The system size is 256×256 and we use the periodic boundary condition in both directions.

duces some monomer mobility? Specifically, here, we allow only hops to NN empty sites at rate $h=h_{1\mathrm{NN}}$. We perform simulations for a range of h, and determine the ordering and percolation transition points using the procedure described in the previous section. The results show that the gap decreases, as h increases. See Table II for a list of transition coverages for various h estimated from a 64×64 system. Note that for even larger values of h, θ_p thus determined can be less than θ_c, but this is due to the finite-size effect. We argue that there exists a critical hopping rate above which the two transitions coincide.

For the purpose of illustration, in Fig. 12 we plot for $h=0$ and $h=0.1p$ both the normalized fluctuations of the order parameter, $\langle m^2\rangle/\theta^2$, and the normalized average size, $\langle s_{\mathrm{av}}\rangle/(L^2\theta)$, of 2nd NN particle clusters as a function of the coverage θ. The gap between the curves for $h=0$ disappears when h increases to above $0.1p$, indicating coincidence. Based on these observations, together with the results in Table II, we argue that the two transitions coincide when the monomer mobility equals $h=0.1p$ or higher. Furthermore, we postulate that at the point where the transitions first coincide, the critical behavior is that of the ''Ising droplets,'' i.e., $\gamma_p=\gamma=7/4$, $\nu_p=\nu=1$, and so on.

VI. DISCUSSION

It is appropriate to provide a more general and intuitive picture of such issues as the existence of a gap between

TABLE II. Ordering and percolation transition coverages for the adsorption-desorption model with different NN hopping rates h. Transition coverages are obtained numerically by requiring the cumulant $Q(\theta_c)=Q_c$ for the ordering transition and the spanning probability $R(\theta_p)=1/2$ for the percolation transition. Results are based on simulations on a 64×64 lattice.

h/p	0.018	0.034	0.049	0.063	0.076
θ_c	0.301	0.304	0.306	0.308	0.310
θ_p	0.306	0.307	0.308	0.309	0.310

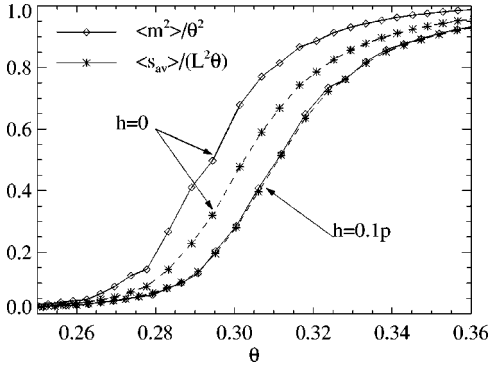

FIG. 12. $\langle m^2\rangle/\theta^2$ and $s_{\mathrm{av}}/(L^2\theta)$ versus θ for 2nd NN clusters when $h=0.1p$ and $h=0$ for a 64×64 system.

ordering and percolation, as well as of the above transition behavior. A basic feature controlling behavior is that percolation cannot occur before symmetry breaking. If in some model symmetry breaking occurs at a ''low'' coverage, then it provides no impediment to percolation which would occur later at some ''natural'' higher coverage (dependent on the connectivity rule). However, if symmetry breaking occurs at a coverage higher than this natural coverage, then it delays percolation, which will likely occur as soon as possible, i.e., coincident with the symmetry breaking.

How can one assess the natural coverage for percolation? One simplistic possibility is to consider models for $c(2\times2)$ ordering where symmetry is ''completely broken'' for all coverages (due to population of just one sublattice), and thus provides no impediment to percolation. In the simplest case, if one sublattice is populated at random, one has $\theta_p^{2\mathrm{NN}}=0.296$, and $\theta_p^{3\mathrm{NN}}=0.204$ (or $\theta_p^{2\mathrm{NN}}=0.281$, and $\theta_p^{3\mathrm{NN}}=0.217$ if one sublattice is populated by irreversible random adsorption of dimers onto 2nd NN sites).[37] For the HS model, the symmetry-breaking transition always occurs well above the natural coverage for percolation of $c(2\times2)$ domains with either 2nd or 3rd NN connectivity. This explains why these transitions are always coincident. For the adsorption-desorption model with zero monomer mobility, this picture applies only for 3rd NN connectivity. In contrast, symmetry breaking occurs at a coverage comparable to the natural coverage for percolation of $c(2\times2)$ domains with 2nd NN connectivity. Thus, it is not surprising that there is a small gap between the corresponding percolation transition and the ordering transition, and that this gap disappears with the introduction of monomer mobility (which delays the symmetry-breaking transition to higher coverages).

Another perspective comes from our site-bond correlated percolation study in Sec. III D. The idea is that we can approximate critical configurations of the nonequilibrium model by those of the hard-square model, but with some particles missing. What is the maximum fraction of particles that can be removed such that this state still percolates? The coverage of remaining particles should roughly correspond to the natural coverage, or to the coverage where percolation and symmetry breaking first coincide (as in Sec. V). Now, the site-bond correlated percolation problem with bond activity p can be crudely approximated by a diluted site percolation problem in which only a fraction of $q=p^{1/2}$ of particles are activated.[38] Then, using the critical bond activity p_c, from Sec. III D, one obtains an estimate for this natural

coverage of $\theta_{\rm nat}=q_c\theta_c^{\rm HS}=p_c^{1/2}\theta_c^{\rm HS}\approx 0.308$ for 2nd NN connectivity. This is consistent with the behavior shown in Fig. 12.

VII. SUMMARY

We have introduced a broad class of nonequilibrium adsorption-desorption models with $c(2\times 2)$ ordering, which include the equilibrium hard-square model as a special case. A comprehensive analysis is provided of the ordering and percolation transitions, and of the relationship between them. The ordering transition is always in the Ising universality class. Typically, percolation coincides with the ordering transition. However, if ordering occurs at sufficiently ''low'' coverages, then there can be a ''gap'' with percolation occurring at a higher coverage. Random percolation universality applies only in the latter case.

ACKNOWLEDGMENTS

This work was supported by the Division of Chemical Sciences, BES, of the U.S. Department of Energy (U.S. DOE). It was performed at Ames Laboratory which is operated for the U.S. DOE by ISU under Contract No. W-7405-Eng-82.

APPENDIX A: STEADY-STATE BEHAVIOR AS $u\rightarrow 1$

Here, we consider in more detail behavior in the limit $u\rightarrow 1$ for the adsorption-desorption model where only hops to NN empty sites are allowed at rate h (measured in units of p). While for the HS model, one has $\theta(u\rightarrow 1)\approx 1/2$ (the maximum possible value), it has been shown previously[18,39] that for $h=0$, one has $\theta(u\rightarrow 1)\approx 0.4253$. The feature that $\theta(u\rightarrow 1)$ is strictly less than 1/2 applies more generally for finite h. This can be understood as follows. In the limit $u\rightarrow 1$, monomer desorption is much slower than all other processes. This means that any empty eight-site ensemble, created by desorption, is filled before subsequent desorption events. However, desorption of monomers produces isolated ''defects'' or vacancies within $c(2\times 2)$ domains, which are ''frozen'' given the above restrictive hopping dynamics. Consequently, they cannot be immediately filled by dimer adsorption. Thus, as $u\rightarrow 1$, one obtains ''jammed'' states which contain no eight-site ensembles, but for which a finite density of isolated defects persists.[39] In contrast, for the HS model, one has $\theta(u\rightarrow 1)\approx 1/2$ simply because the density of eight-site ensembles is nonzero for any coverage strictly below 1/2.

For finite h, we simulate the $u\rightarrow 1$ limit directly using the following algorithm. Starting from a perfect $c(2\times 2)$ adlayer (or any ''jammed'' state), we randomly remove a monomer from the surface. We then test whether it is possible to deposit dimers, *or* for monomers to hop on the surface. If so, we attempt the two processes with their respective rates, until no further deposition *or* hopping is possible. Then, we proceed with removal of another monomer, continuing until a steady state is achieved. We find that $\theta(u\rightarrow 1)=0.4253$, 0.4274, 0.4320, 0.4336, 0.4343, . . . for $h=0$, 1, 16, 128, 1024, . . . , respectively, i.e., $\theta(u\rightarrow 1)$ increases as h increases, albeit very slowly. Unfortunately simulation with very large h is difficult, and we cannot definitively conclude whether $\theta(u\rightarrow 1)$ reaches 1/2, as $h\rightarrow\infty$.

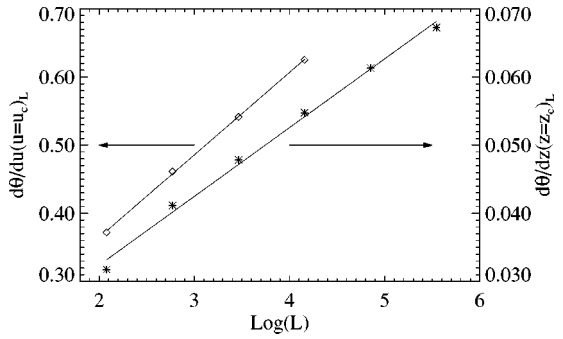

FIG. 13. Left: dependence of $d\theta/du$ at u_c on the system size L for the nonequilibrium model with $h_{\rm iNN}=0$. Right: $d\theta/dz$ at z_c for the hard-square model.

For $u<1$, the adsorption-desorption model should recover HS model behavior as $h\rightarrow\infty$, provided there is no blocking transition (as was previously conjectured[21]). The existence of a blocking transition for the ''jammed'' states of the $u\rightarrow 1$ limit has not been considered previously. Despite the slow increase of $\theta(u\rightarrow 1)$ for large h, we do not have any definitive evidence for its existence.

APPENDIX B: SINGULARITY IN THE STEADY-STATE COVERAGE AT u_c

We wish to determine the nature of any singularity in the coverage θ as a function of u at the ordering transition in our adsorption-desorption model. One generally expects the following scaling form:

$$\theta-\theta_c\sim(u-u_c)^{1-\alpha}, \tag{B1}$$

where α is a critical exponent, which is related to the specific heat for an equilibrium model. We define all the exponents using u as the control parameter, e.g., $\langle m\rangle\sim(u-u_c)^{\beta}$. Then, for the corresponding exponents using θ instead of u, Fisher's renormalization[40] gives

$$\beta_\theta=\beta/(1-\alpha),\quad \gamma_\theta=\gamma/(1-\alpha), \tag{B2}$$

and so on. What is α for our model? We know that for the Ising universality class $\alpha=0$, implying only logarithmic singularities. If $d\theta/du\sim\log|u-u_c|$, as $u\rightarrow u_c$, we can assume the following finite-size scaling form:

$$d\theta/du\approx A\log L+F((u-u_c)L^{1/\nu}). \tag{B3}$$

Simulation results for immobile monomers (Fig. 13) are consistent this conjecture.

We performed a similar analysis for the HS model, but more conventionally using z (rather than u) as the control parameter. Our results again suggest that $\alpha=0$ (Fig. 13). Myshlyavtsev *et al.*[41] studied this exponent for a lattice-gas model with finite repulsive NN interactions at a temperature corresponding to about 60% of the Onsager point. Using the transfer-matrix technique, they fit the maximum value of $\partial\theta/\partial\mu$ to $A+BL^{\lambda}$ (where μ is the chemical potential). They find that $\lambda\approx 0.2$ at $L=16$ but there is a trend of decreasing λ as L increases, consistent with a logarithmic divergence.

APPENDIX C: CLUSTER ALGORITHM AND HISTOGRAM ANALYSIS

In their seminal work, Swendsen and Wang[2] introduced cluster dynamics algorithms to alleviate difficulties with critical slowing down in Monte Carlo simulations. Recently, some refined algorithms for hard-core particles have been developed (see Ref. 42 and references therein). These replace the spin-flip operation in the original Swendsen-Wang algorithm with certain geometric operations (rotation, reflection about a line, etc.). In this appendix, we briefly describe the algorithm for the hard-square model used in this work.

Let $\{n_A\}$ denote a configuration of the hard-square model, and $\{n_B\}$ the configuration obtained through reflection about a line. If we superimpose $\{n_A\}$ upon $\{n_B\}$, some of the particles will overlap (representing particles by hard squares with a side length of $\sqrt{2}$ lattice units and rotated by 45°). We can define a corresponding new kind of connectivity: if particle i from $\{n_A\}$ and particle j from $\{n_B\}$ overlap, then i and j are connected. The usual Hoshen-Kopelman labeling technique can be applied to classify clusters. Typically, a cluster thus defined will have a mirror image, except in cases when the mirror image is itself. Our dynamics algorithm flips half these pairs of clusters (chosen at random) at each step (so that if a cluster is flipped, so is its mirror image). It is easy to see that this operation does not violate the NN exclusion rule. Detailed balance is satisfied trivially, and the ergodicity can be argued following Wolff.[43]

To overcome critical slowing down in the HS model, we want to speed up the fluctuations in the populations of particles in the two sublattices. Therefore, in the above algorithm, we choose the reflection operation about a line at half lattice locations, so that a particle from the + sublattice will be mapped into the − sublattice through a reflection operation. We also choose the direction (along the two principal axes) and the position of this line randomly.

Ferrenberg *et al.*[44] show that some so-called high-quality pseudorandom number generators (PNG) can give erroneous results when a pure cluster algorithm is used. Thus, in our simulations, we interpose a regular Metropolis-type MC sweep (involving adsorption or desorption of monomers) between every cluster operation, which is believed to mitigate any defect in the PNG. Unlike the cluster flip operation, the usual MC sweep can change the number of particles. For the PNG, we use a combination of a subtractive Fibonacci, a shift register, and a linear congruential generator.[45]

To test the reliability of the cluster algorithm, we determine from simulation in a small 6×6 site system, the fraction of configurations with n particles. Values are consistent with results obtained by exact enumeration.

[1] *The Monte Carlo Method in Condensed Matter Physics*, 2nd ed., edited by K. Binder, Topics in Applied Physics Vol. 71 (Springer, Berlin, 1995).
[2] R. Swendsen and J.-S. Wang, Phys. Rev. Lett. **58**, 86 (1987).
[3] K. K. Murata, J. Phys. A **12**, 81 (1979).
[4] A. Coniglio and W. Klein, J. Phys. A **13**, 2775 (1980).
[5] A. L. Stella and C. Vanderzande, Phys. Rev. Lett. **62**, 1067 (1989).
[6] A. Coniglio, F. di Liberto, and G. Monroy, J. Phys. A **14**, 3017 (1981).
[7] A. Coniglio, F. di Liberto, G. Monroy, and F. Peruggi, Phys. Lett. **87A**, 189 (1982).
[8] G. Giacomin, J. L. Lebowitz, and C. Maes, J. Stat. Phys. **80**, 1379 (1995).
[9] J. Marro and R. Dickman, *Nonequilibrium Phase Transitions in Lattice Models, Collection Aléa-Saclay. Monographs and Texts in Statistical Physics* (Cambridge University Press, Cambridge, 1999).
[10] J. J. Alonso, A. I. López-Lacomba, and J. Marro, Phys. Rev. E **52**, 6006 (1995).
[11] M. Chaves and M. A. Santos, Physica A **262**, 420 (1999).
[12] Z. Ràcz, Phys. Rev. B **21**, 4012 (1980).
[13] D. W. Wood and M. Goldfinch, J. Phys. A **13**, 2781 (1980).
[14] G. Kamieniarz and H. W. J. Blöte, J. Phys. A **26**, 6679 (1993).
[15] C.-K. Hu and K.-S. Mak, Phys. Rev. B **39**, 2948 (1989).
[16] V. P. Zhdanov and B. Kasemo, Surf. Sci. **412/413**, 527 (1998).
[17] Y. Suchorski, J. Beben, E. W. James, J. W. Evans, and R. Imbihl, Phys. Rev. Lett. **82**, 1907 (1999).
[18] E. W. James, C. Song, and J. W. Evans, J. Chem. Phys. **111**, 6579 (1999).
[19] D.-J. Liu and J. W. Evans, Phys. Rev. Lett. **84**, 955 (2000).
[20] A. B. Bortz, M. H. Kalos, and J. L. Lebowitz, J. Comput. Phys. **17**, 10 (1975).
[21] W. Ertel, K. Froböse, and J. Jäckle, J. Chem. Phys. **88**, 5027 (1988).
[22] J. W. Essam, in *Phase Transitions and Critical Phenomena*, edited by C. Domb and M. S. Green (Academic Press, London, 1972), Vol. 2, pp. 197–270.
[23] J. W. Evans, Rev. Mod. Phys. **65**, 1281 (1993).
[24] D. S. Gaunt and M. E. Fisher, J. Chem. Phys. **43**, 2840 (1965).
[25] K. Binder and D. P. Landau, Phys. Rev. B **21**, 1941 (1980).
[26] R. J. Baxter, I. G. Enting, and S. K. Tsang, J. Stat. Phys. **22**, 465 (1980).
[27] F. H. Ree and D. A. Chesnut, J. Chem. Phys. **45**, 3983 (1966).
[28] R. Q. Hwang, E. D. Williams, N. C. Bartelt, and R. L. Park, Phys. Rev. B **37**, 5870 (1988).
[29] H. W. J. Blöte and X.-N. Wu, J. Phys. A **23**, L627 (1990).
[30] C. Dress and W. Krauth, J. Phys. A **28**, L597 (1995).
[31] K. Binder, Z. Phys. B: Condens. Matter **43**, 119 (1981).
[32] A. M. Ferrenberg and R. H. Swendsen, Phys. Rev. Lett. **63**, 1195 (1989).
[33] G. Kamieniarz and H. W. J. Blöte, J. Phys. A **26**, 201 (1993).
[34] R. M. Ziff, Phys. Rev. Lett. **69**, 2670 (1992).
[35] P. J. M. Bastiaansen and H. J. F. Knops, J. Phys. A **30**, 1971 (1997).
[36] C. Vanderzande and A. L. Stella, J. Phys. A **22**, L445 (1989).
[37] These thresholds equal one-half of the values for random percolation (or random sequential adsorption of dimers on to NN sites) on a square lattice. See Ref. 23.
[38] The relation $p=q^2$ comes from activating a bond between to particles if they are both active. However, this creates correlations between active bonds, which are absent in the analysis of Sec. III D. To avoid this complication, one could modify the analysis of Sec. III D to introduce random site (rather than bond) dilution, and directly determine q_c.

[39] E. W. James, D.-J. Liu, and J. W. Evans, Colloids Surf., A **165**, 241 (2000).
[40] M. E. Fisher, Phys. Rev. **176**, 257 (1968).
[41] A. V. Myshlyavtsev, A. A. Stepanov, C. Uebing, and V. P. Zhdanov, Phys. Rev. B **52**, 5977 (1995).
[42] H. W. J. Blöte and J. R. Heringa, in *Computer Simulation Studies in Condensed-Matters Physics X*, edited by D. P. Landau, K. K. Mon, and H.-B. Schüttler, Springer Proceedings in Physics Vol. 83 (Springer-Verlag, Berlin, 1998), p. 53.
[43] U. Wolff, Phys. Rev. Lett. **62**, 361 (1989).
[44] A. M. Ferrenberg, D. P. Landau, and Y. J. Wong, Phys. Rev. Lett. **69**, 3382 (1992).
[45] W. H. Press, S. A. Teukolsky, W. T. Vettering, and B. P. Flannery, in *Numerical Recipes in Fortran 90*, 2nd ed. (Cambridge University Press, Cambridge, 1996), Chap. B7.